LETTERS

The Mesp2 transcription factor establishes segmental borders by suppressing Notch activity

Mitsuru Morimoto[1], Yu Takahashi[3], Maho Endo[1] & Yumiko Saga[1,2]

The serially segmented (metameric) structures of vertebrates are based on somites that are periodically formed during embryogenesis. A 'clock and wavefront' model has been proposed to explain the underlying mechanism of somite formation[1], in which the periodicity is generated by oscillation of Notch components (the clock) in the posterior pre-somitic mesoderm (PSM)[2–6]. This temporal periodicity is then translated into the segmental units in the 'wavefront'[7,8]. The wavefront is thought to exist in the anterior PSM and progress backwards at a constant rate; however, there has been no direct evidence as to whether the levels of Notch activity really oscillate and how such oscillation is translated into a segmental pattern in the anterior PSM. Here, we have visualized endogenous levels of Notch1 activity in mice, showing that it oscillates in the posterior PSM but is arrested in the anterior PSM. Somite boundaries formed at the interface between Notch1-activated and -repressed domains. Genetic and biochemical studies indicate that this interface is generated by suppression of Notch activity by mesoderm posterior 2 (Mesp2) through induction of the lunatic fringe gene (*Lfng*). We propose that the oscillation of Notch activity is arrested and translated in the wavefront by Mesp2.

Mesp2—a basic helix–loop–helix-type transcription factor—and its related proteins have an essential role in both segmentation and rostro-caudal patterning of somites in the anterior PSM[9–12]. To understand further the involvement of Mesp2 in boundary formation, we generated a *Mesp2–venus* knock-in mouse (Supplementary Fig. 1) in which Mesp2 localization is detected in live embryos using confocal microscopy (Fig. 1a–g). As expected, the Mesp2–venus fusion protein was detected in the nuclei of cells (Fig. 1d). Furthermore, in embryos at 8.75 days post coitus (d.p.c.), two to three segmental stripes are detectable, showing an anterior to posterior gradient for each segment (Fig. 1a–d). The signal in the most anterior segment is very weak but a second stripe has a clear anterior boundary that perfectly matches the segmental border; indeed, it lines the entire border. The strongest third stripe also has a clear anterior border in the PSM in which no sign of a morphological boundary can be detected. This band may therefore demarcate the next segmental border. In later-stage embryos, one clear stripe was detected, although we occasionally observed an additional signal in the newly formed somite (Fig. 1e– g).

We have previously shown that the expression domain of *Mesp2* transcript changes during somitogenesis[13], appearing at S−1 or S−2 as a single band of one somite in length, and then gradually shrinking, leaving the rostral half of its expression domain intact. To elucidate further the dynamic behaviour of Mesp2, we have recorded its expression pattern using time-lapse microscopy. A new Mesp2 expression domain is evident as a single band of about one somite in length, whereas the expression domain of the pre-existing band undergoes changes such that the rostral part of the band is maintained longer before finally disappearing (Supplementary Movie 1 and Supplementary Fig. 2). This dynamic change is consistent with the expression profile of *Mesp2* messenger RNA, previously obtained using explant cultures[13]. However, because Mesp2–venus is a fusion protein, it may not faithfully reproduce the pattern of endogenous protein distribution. This prompted us to generate antibodies against the Mesp2 protein. The antibody-staining pattern reveals that the distribution of endogenous Mesp2 is similar to that of Mesp2–venus (Fig. 1h–j). The neighbouring section was subjected to *in situ* hybridization analysis. The mRNA localization pattern was found to be consistent with the immunohistochemical results, indicating that message is translated immediately and that the protein is rapidly degraded but the transcript disappears earlier, as expected (Fig. 1j). We occasionally observed two bands of Mesp2 protein: an anterior band located in the segmented border and an posterior one in the next presumptive border. In this case, transcript was only observed in the posterior region (Fig. 1h). Taken together, we conclude that the anterior border of the expression domain of the Mesp2 protein coincides with the next segmental border in the PSM.

The expression of Notch components, such as *Hes7* (hairy and enhancer of split 7) and *Lfng*, oscillates in the PSM[3,4,6], whereas *Notch1* is expressed throughout the entire PSM and at higher levels in the anterior PSM[9]. We attempted to visualize the activation of Notch signalling by detecting a processed NICD (Notch intracellular domain) using a specific antibody. Unlike its RNA expression pattern, Notch1 activity exhibits a dynamic pattern in the PSM during somitogenesis. We analysed 52 embryos, which exhibited four distinct patterns; the positive signals were detected in the tailbud (Fig. 1k), the middle of the PSM (Fig. 1l, m) or more anteriorly within the PSM (Fig. 1n). Notably, in most of the embryos, Notch activation is in a similar phase to the transcript of *Lfng*, which encodes a glycosyltransferase that can modify Notch activity[14,15] (Fig. 1k–n). The expression domain of *Lfng* appears slightly later than Notch activation, supporting the idea that *Lfng* transcription is activated by Notch signalling, as previously indicated[16]. These results indicate that the activity of Notch oscillates in the posterior PSM. In a previous report, Hes7 was shown to function as a suppressor of *Hes7* and *Lfng* transcription[17], forming a feedback loop in the core oscillator. We thus tested the pattern of Notch activation in mice defective in Notch pathway components (Fig. 2a–e). In *Dll1*-null embryos[18], no Notch1 activity is found anywhere in the PSM (Fig. 2c), whereas in *Lfng*-null embryos[19], Notch1 activity is detected throughout the entire PSM but does not seem to oscillate (Fig. 2d). These observations indicate that the Dll1 ligand is required for Notch1 activation, and that Lfng functions as a suppressor of Notch activity, thus generating the oscillatory activation of Notch1.

In the anterior PSM, Notch oscillatory activity is arrested and localizes in the caudal portion of the S0 somite, whereas *Lfng* transcripts are detectable in the rostral part of S − 1 and their

[1]Division of Mammalian Development, National Institute of Genetics, and [2]Sokendai, Yata 1111, Mishima 411-8540, Japan. [3]Cellular & Molecular Toxicology Division, National Institute of Health Sciences, 1-18-1 Kamiyoga, Setagaya-ku, Tokyo 158-8501, Japan.

© 2005 Nature Publishing Group

expression seldom overlaps with the Notch1 activation domain (Fig. 1k–n). Of note, Notch activation and *Lfng* expression domains almost co-occur in the posterior PSM, but are segregated into the rostral and caudal parts in the anterior PSM. This suggests that *Lfng* expression is activated by an additional factor in the anterior PSM. Mesp2 may well be this factor, as it is co-expressed with *Lfng* in this region (refs 20, 21; see also Supplementary Fig. 3). We propose that in the anterior PSM, Mesp2 may downregulate Notch activity through the activation of Lfng, which is a Notch modulator. To address this possibility, we first examined the relationship between Mesp2 and Notch activity in the anterior PSM. Double staining with anti-active-NICD and anti-Mesp2 antibodies enabled us to examine the spatial relationship between the localization of these two factors in a single section (Fig. 2f–u). At the initial phase of Mesp2 expression the two expression domains partially overlap in such a way that cells in the posterior Notch activation domain co-express Mesp2 (Fig. 2f–i). The overlapping domain gradually reduces as expression levels of Mesp2 increase (Fig. 2j–m). Ultimately, the two expression domains are completely separated from each other and form a clear boundary (Fig. 2n–q). Notably, the strongest detectable signals of both Notch activity and Mesp2 are found in close proximity to the boundary on both sides. This boundary will form the next segmental border, as indicated by the expression of Mesp2–venus (Fig. 1a–g). Once a new border is generated, next Notch activity appears in the anterior PSM and Mesp2 protein appears just in the middle of the Notch activation domain, to generate a next segmental border (Fig. 2r–u).

We next examined whether downregulation of Notch activity by Mesp2 is mediated by Lfng. In *Lfng*-null embryos[19], Mesp2 protein is

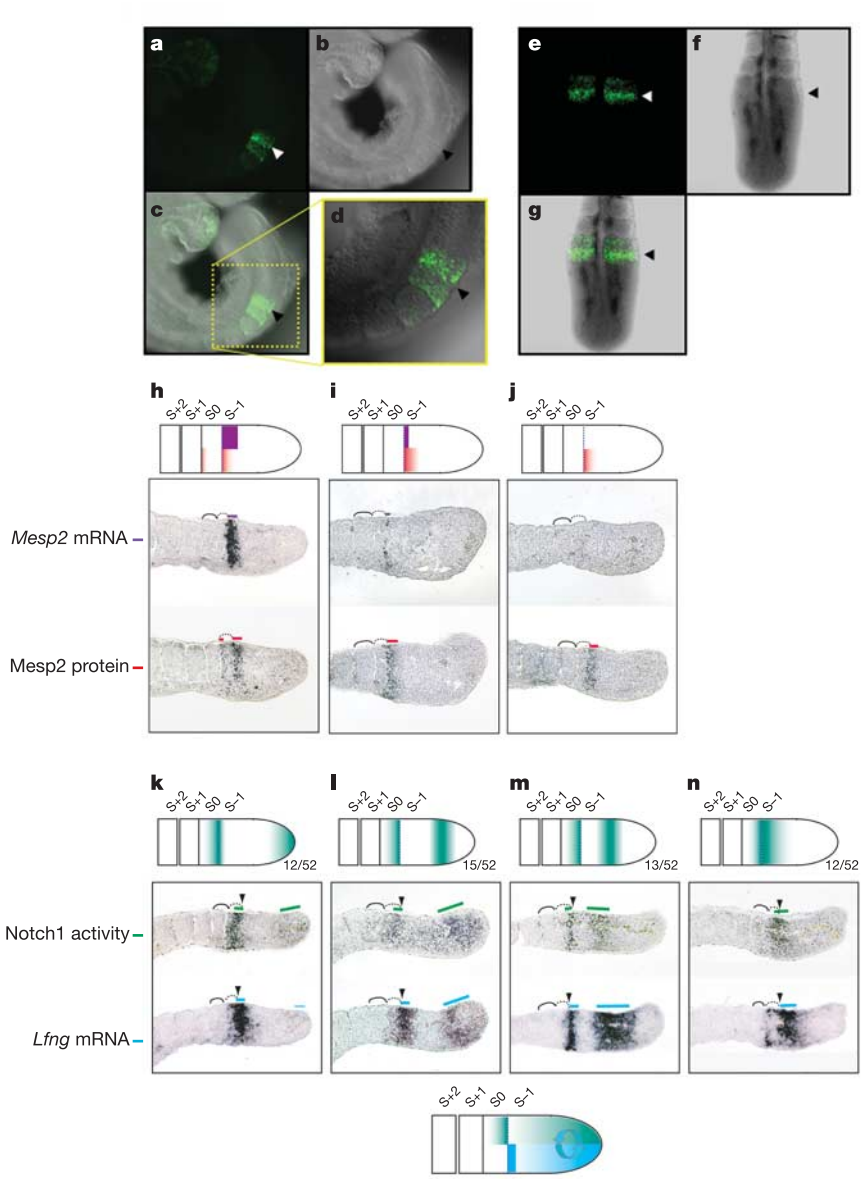

Figure 1 | Visualization of the Mesp2 protein and oscillation of Notch1 activity and *Lfng* transcripts. **a**–**g**, Expression of the Mesp2–venus fusion protein is shown in 8.75 d.p.c. (**a**–**d**) and 10.5 d.p.c. (**e**–**g**) embryos as confocal images (**a**, **e**; green), bright-field images (**b**, **f**) and merged images (**c**, **g**). The boxed area in **c** is shown at higher magnification in **d**. Stronger Mesp2–venus signals are localized at the anterior border of the predicted next somite (next borders are indicated by arrowheads). **h**–**j**, *Mesp2* transcript and protein (using anti-Mesp2 antibody) expression was compared using three sets of serial sections of 11.5 d.p.c. embryos. **k**–**n**, Notch1 activity periodically oscillating in the PSM may activate *Lfng* transcription. Notch1 activity was revealed by immunostaining with antibodies against active-NICD and the adjacent sections were stained by *in situ* hybridization with *Lfng* probe. Solid and dotted lines indicate S+1 and S0 somite regions, respectively, and coloured bars represent the stained domain. $n = 52$ embryos. Each expression pattern is summarized on the top of each panel.

© 2005 Nature Publishing Group

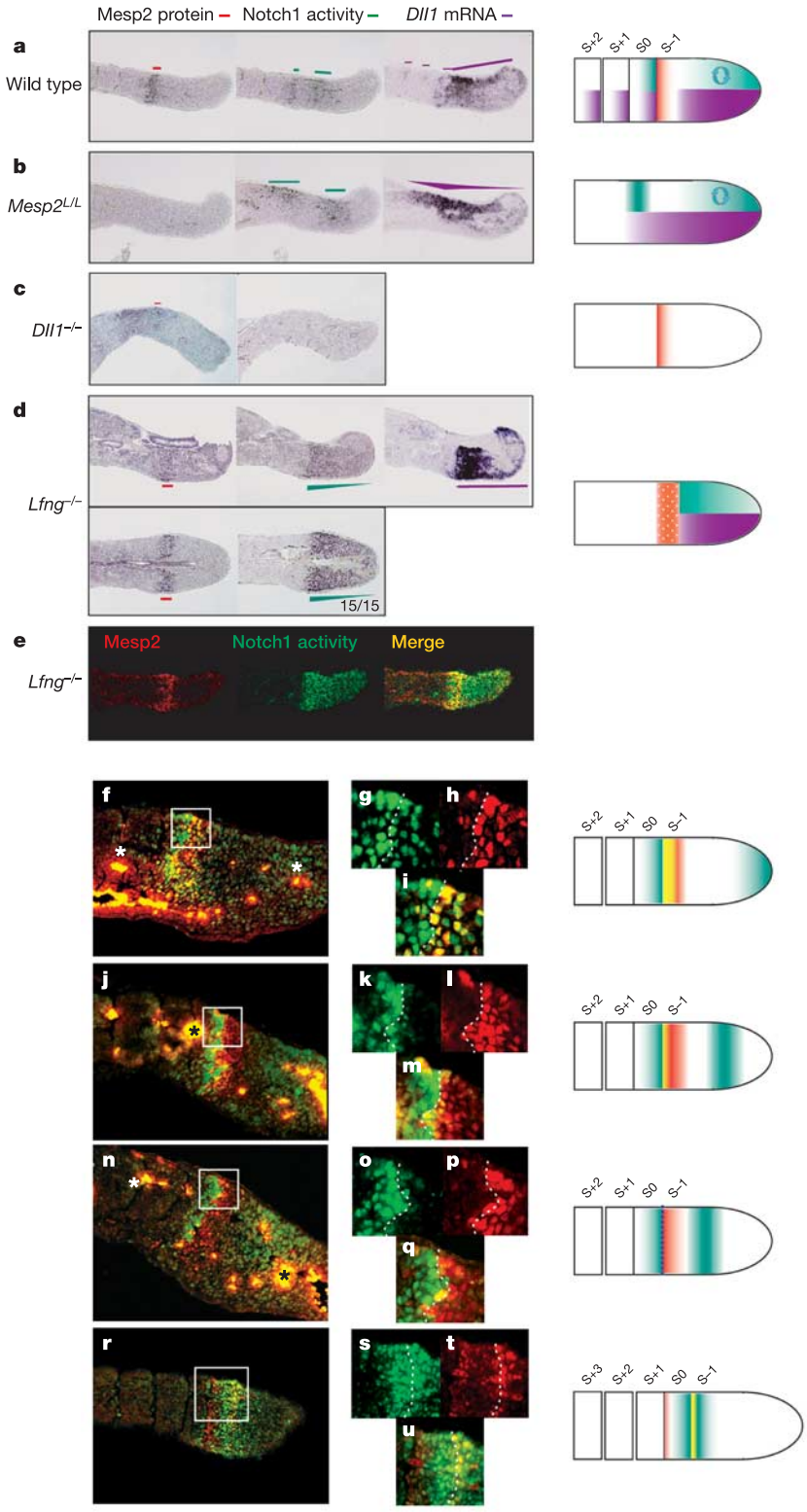

Figure 2 | Analyses of gene and protein expression critical for clock oscillation and its arrest. **a**–**e**, Serial sections were prepared from 11.5 d.p.c. wild type (**a**), *Mesp2*$^{L/L}$ (**b**), *Dll1*$^{-/-}$ (**c**) or *Lfng*$^{-/-}$ (**d**, **e**) embryonic tails. Each section was stained with anti-Mesp2 or anti-active-NICD antibodies, or with *Dll1* or *Lfng* RNA probe. Coloured bars represent stained domains. In *Mesp2*$^{L/L}$ embryos, Notch1 activity is expanded in the anterior PSM, and expression of *Dll1* is also strongly expanded. In *Dll1*$^{-/-}$ embryos, expression of Mesp2 is decreased and Notch1 activity is almost completely lost. In all *Lfng*$^{-/-}$ embryos ($n = 15$), Notch1 activity is strongly detected throughout the PSM but its oscillatory expression is lost. Each expression pattern is summarized in the right panels. **f**–**u**, Mesp2 protein (red) and Notch1 activity (green) were compared by double immunostaining. A merged set of four images representing different patterns is shown (**f**, **j**, **n**, **r**). The border regions (boxed areas) are magnified and the signals are shown either separately (**g**, **h**, **k**, **l**, **o**, **p**, **s**, **t**) or merged (**i**, **m**, **q**, **u**). Dotted lines indicate the boundaries, and the expression patterns are summarized in the right panels. Asterisk indicates nonspecific immunofluorescence of blood cells.

© 2005 Nature Publishing Group

expressed in the appropriate location, although the expression is broad and does not show a normal anterior–posterior gradient (Fig. 2d). Hence, Lfng is required for normal Mesp2 protein localization. Importantly, the anterior limit of the Notch1 activation domain, which encompasses the PSM and does not have oscillatory Notch1 activity, overlaps with the Mesp2 expression domain, indicating that Mesp2 fails to suppress Notch activity and thus the Notch activation domain does not segregate in *Lfng*-null embryos (Fig. 2d, e).

To study further the function of Mesp2 in the control of both Notch activity and *Lfng* expression, a number of neighbouring sections of *Mesp2*-null embryos were subjected to NICD and *Lfng* staining. We observed that Notch1 activity and *Lfng* expression oscillate normally in the posterior PSM in *Mesp2*-null embryos; however, their expression is abnormal and expands anteriorly in the anterior PSM, and they do not make narrow stripes (Fig. 3a). This was more clearly shown in whole-mount staining of *Lfng* expression in 9.5 d.p.c. embryos (Supplementary Fig. 4). The expanded signals could be sustained by ectopic expression of *Dll1*, which extends anteriorly in *Mesp2*-null embryos (Fig. 2b and ref. 9). More importantly, the two domains of Notch1 activation and *Lfng* expression are never segregated and stay in unison (compare Figs 1k–m and 3a). We interpret this to mean that in wild-type embryos, Mesp2 disrupts the relationship between Notch activity and Lfng by stably activating Lfng, a Notch repressor, in the anterior PSM. In order to determine whether Mesp2 acts on the *Lfng* enhancer and regulates its gene expression, we generated a reporter construct that contained a 2.3-kilobase (kb) upstream enhancer sequence (defined by transgenic analyses reported in refs 20 and 21) linked to a luciferase gene (Fig. 3b). As shown in Fig. 3c, both Mesp2 and NICD act as activators in this reporter system, and a synergistic effect was also observed. However, these activities are strongly suppressed by Hes7, which is active in the posterior PSM and is downregulated in the anterior PSM[22]. Furthermore, we found that Mesp2 specifically binds to a portion of the *Lfng* enhancer that contains a putative N-box (Fig. 3d). These results strongly suggest that *Lfng* is activated by NICD and suppressed by Hes7 in the posterior PSM, whereas it is activated by Mesp2 and hence its expression is restricted and confined to the Mesp2 expression domain, thereby inhibiting and arresting the oscillation of Notch activity (Fig. 4 and ref. 16). This

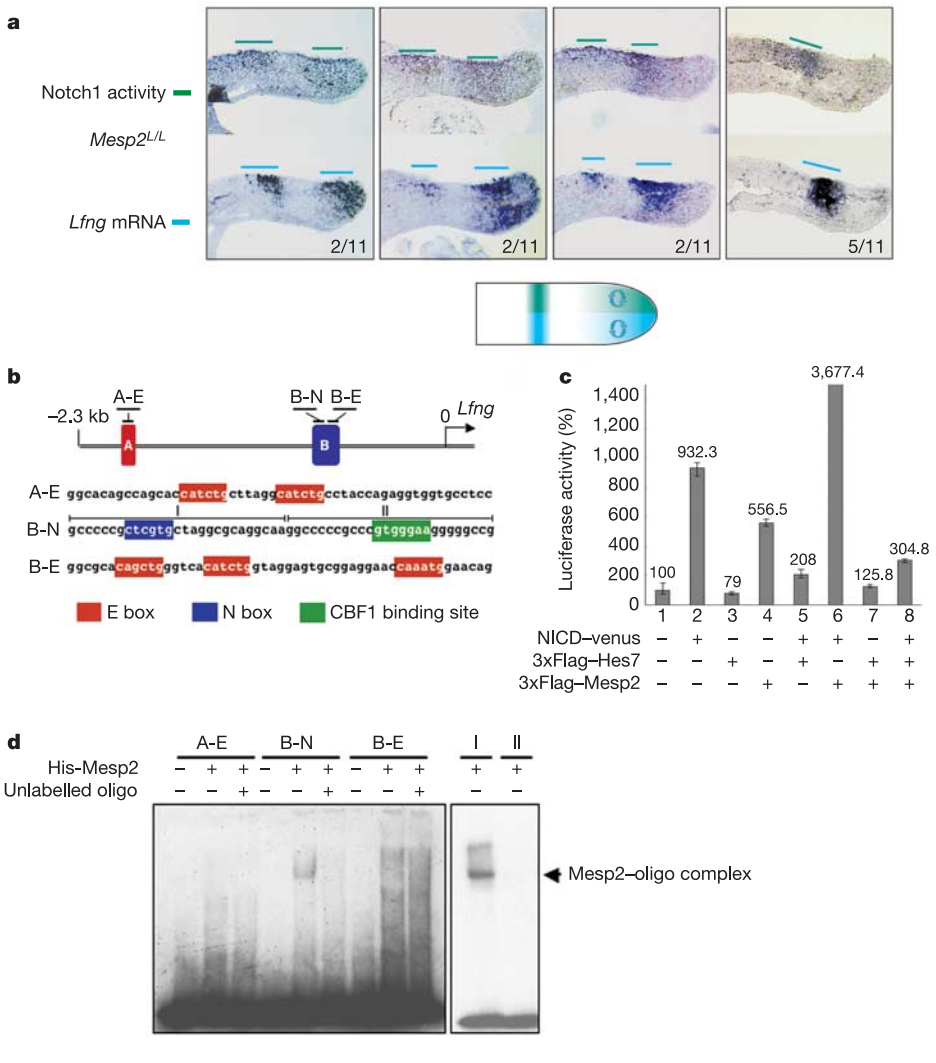

Figure 3 | Mesp2 may activate *Lfng* to arrest the oscillation of Notch activity in the anterior PSM. a, Serial sections of mouse tail regions were prepared from *Mesp2*$^{L/L}$ embryos ($n = 11$) and stained with either anti-active-NICD antibody (top) or *Lfng* probe (bottom). Notch1 activity and *Lfng* signal oscillate in the posterior PSM but do not arrest in the anterior PSM. **b**, A schematic representation of a luciferase reporter construct with an *Lfng* 5′ upstream region (top). DNA fragments A-E, B-N and B-E are used for gel mobility shift assays. **c**, Luciferase reporter assay showing that NICD and Mesp2 are strong activators of the *Lfng* enhancer, whereas Hes7 is a strong repressor of the *Lfng* enhancer. **d**, Mesp2 specifically binds only to the N-box-containing B-N fragment.

© 2005 Nature Publishing Group

result is consistent with previous studies indicating that the regulatory region of *Lfng* is separable into a region A that regulates the cyclic expression in the posterior PSM, and a region B that regulates expression in the anterior PSM[20,21].

The PSM can be divided into two regions based on the finding that the clock oscillates in the posterior PSM whereas it is slowed down and arrested in the anterior PSM. A switch between these two states is thought to be triggered by FGF signalling[23,24], and Mesp2 is crucial in this process. In the absence of Mesp2, the Dll1-dependent relationship between Notch activity and Lfng is maintained; that is, the normal wavefront is not generated, even if the clock system functions normally. We have previously shown that a major role of Mesp2 is to generate rostro-caudal polarity within the somite through suppression of the Dll1-dependent Notch pathway in the presumptive rostral domain[13]. We now propose that Mesp2 has an additional role in segment border formation by restricting *Lfng* expression in the anterior PSM. In both cases, Mesp2 functions as a strong suppressor of Notch activity.

We have shown that Lfng is a negative regulator of Dll1–Notch signalling. The results are consistent[16] or contrast[25,26] with previous findings. In the *Drosophila* wing disc, Fringe inhibits Serrate-dependent but potentiates Delta-dependent Notch signalling, whereas in somite segmentation, Lfng suppresses Dll1-dependent Notch activation (Fig. 4 and ref. 16). In a mammalian cell culture system, Dll1–Notch signalling is enhanced by Lfng[27]. These discrepancies could be due to different cellular contexts and different biological systems, emphasizing variation of modulating mechanisms for Notch signalling.

We have now provided direct evidence that Notch activity constitutes a core of the segmentation clock and that Mesp2 arrests the oscillation of Notch activity and initiates a segmentation programme. The next crucial question would be the mechanism by which Mesp2 is turned on in the anterior PSM. Our analyses have revealed a strict spatial relationship between stabilized Notch activation domains and the emergence of Mesp2 expression (Fig. 2f–u; see also Supplementary Fig. 5). In the absence of Notch signalling, however, the Mesp2 expression region is approximately normal in the anterior PSM (Fig. 2c), and thus its initial activation depends on positional information such as the Fgf8 (refs 23, 24) and retinoic acid (RA) gradients[28]. However, the role of RA remains elusive because no severe effect on Mesp2 expression is observed in a targeted disruption of CYP26 (ref. 29), a degrading enzyme of RA (Supplementary Fig. 6). Detailed enhancer analysis of Mesp2 will provide further insights into the mechanism of where and how a sharp NICD–Mesp2 boundary forms.

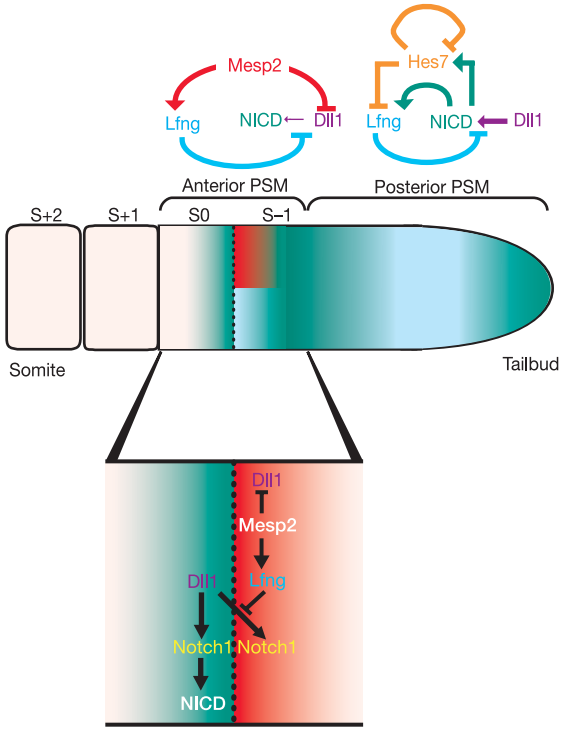

Figure 4 | Schematic representation of the regulatory mechanism underlying the clock system and of the implications of Mesp2 function in establishing the segmental boundary. In the posterior PSM, the Dll1–Notch signal initially activates both *Lfng* and *Hes7*. Hes7 is a strong transcriptional repressor of *Lfng* and of the *Hes7* gene itself, whereas Lfng is a negative modulator of the Notch receptor in this cellular context. The positive and negative feedback loops thus generates oscillation of Notch1 activity. In the anterior PSM, the Notch1 activity and *Lfng* waves are no longer subject to negative regulation by Hes7, as Mesp2 now becomes a major regulator of *Lfng* activation and *Dll1* suppression. As a result, both Notch1 activity and *Lfng* waves are arrested and generate a clear boundary between the Notch1 activity domain and the Mesp2 expression domain, which produce the next segmental boundary.

METHODS

Time-lapse recording using confocal microscopy. Heterozygous Mesp2–venus mouse embryos were collected at 10.5 d.p.c. The tail region was excised and cultured with DMEM/F12 medium (without Phenol red) containing 10% fetal calf serum on a 35-mm glass-bottomed dish (Matsunami Glass) at 37 °C. For the culturing of embryos, the Heating Insert P and Incubator S systems (Zeiss) were used to obtain optimal growth conditions. Scanning for the fluorescence protein venus[30] (excitation at 514 nm) and bright imaging of the tail region was performed with an Axiovert 200M confocal laser scanning microscope (Zeiss). Three-dimensional (x, y, t) image data sets were recorded at 10-min intervals as typical time-lapse imaging sessions ($n = 30$). The colour images were captured using an Axiocam (Zeiss) and converted to pseudo-colours using Zeiss Axiovision software.

***In situ* hybridization and immunohistochemistry.** The tails were dissected at 10.5–11.5 d.p.c., fixed with 4% PFA and embedded in OCT. For *in situ* hybridizations, frozen sections (6–8 μm) were hybridized with digoxigenin-labelled antisense cRNA probes (Roche). Hybridized probes were detected using AP-conjugated anti-DIG sheep antibody (1:1,000, Roche) and visualized with NBT/BCIP (1:50, Roche).

For immunohistochemistry analysis, frozen sections (6–8 μm) were immersed in unmasking solution (Vector Laboratories) and autoclaved at 105 °C for 15 min to enable antigen retrieval. Immunostaining was then performed following a standard method with either anti-Mesp2 (1:500) or anti-NICD (1:500, Cell signaling technology) as primary antibodies, biotinylated anti-rabbit IgG goat antibody (1:200, Vector Laboratories) as a secondary antibody and an ABC kit (Vector Laboratories) for signal detection.

For double-immunofluorescent staining, antibody reactions and the detection of Notch1 activity and Mesp2 were separately conducted after antigen retrieval. Detection of Notch1 activity was performed first with anti-active-NICD (1:200, Cell signaling technology) primary antibody, horseradish peroxidase-conjugated anti-rabbit IgG donkey antibody (1:100, Amersham Pharmacia Biotech) secondary antibody and fluorescein isothiocyanate-conjugated Tyramid (Perkin Elmer) signal detection. Detection of Mesp2 was then performed with anti-Mesp2 (1:200) biotinylated anti-rabbit IgG goat antibody (1:200, Vector Laboratories) and Alexa Flour-594-conjugated Streptavidin (Molecular Probes). The corresponding signals were observed with an Olympus BX61 fluorescence microscope system using an ORCA-ER digital camera (HAMAMATSU photo) and analysed with MetaMorph software (Universal Imaging).

Luciferase assay. For luciferase reporter analysis under the control of the *Lfng* upstream 2.5-kb (*Eco*RI–*Not*I) enhancer (0.2 μg), the reporter construct was transfected with or without the expression vectors for NICD–venus (50 ng), 3 × Flag-tagged Hes7 (20 ng) or 3 × Flag-tagged Mesp2 (50 ng) into NH3T3 cells (0.25×10^5 cells per well in 24-multiwell plates) using Lipofectamine Plus (Invitrogen) following the manufacturer's instructions. The vector containing the Renilla luciferase gene under the control of the thymidine kinase promoter (10 ng) was co-transfected as an internal standard to normalize for transfection efficiency. After 36 h, luciferase activities were measured using a Dual Luciferase Assay Kit (Promega).

Gel-shift assay. A 6 × His-Mesp2 protein was produced using a baculovirus

© 2005 Nature Publishing Group

expression system with Sf-9 cells, and then purified through a TALON metal affinity resin (Clontech) with 100 mM imidazole as the elution buffer. The double-stranded DNA oligonucleotide probes were end-labelled with DIG and protein–DNA complexes were detected using a Roche DIG gel shift kit. Binding reactions were carried out for 30 min on ice, and protein–DNA complexes were analysed on 6% native-polyacrylamide gels. The sense strand sequences of the oligonucleotide probes used were: A-E 5′-GGGCACAGCCAGCACCATCTGCT-TAGGCATCTGCCTACCAGAGGTGGTGCCTCC-3′; B-N 5′-GCCCCCGCT CGTGCTAGGCGCAGGCAAGGCCCCCGCCCGTGGGAAGGGGGCCG-3′; B-E 5′-GGCGCACAGCTGGGTCACATCTGGTAGGAGTGCGGAGGAACC AAATGGAACAG-3′.

Received 3 January; accepted 31 March 2005.

1. Cooke, J. & Zeeman, E. C. A clock and wavefront model for control of the number of repeated structures during animal morphogenesis. *J. Theor. Biol.* **58,** 455–476 (1976).
2. Palmeirim, I., Henrique, D., Ish-Horowicz, D. & Pourquie, O. Avian hairy gene expression identifies a molecular clock linked to vertebrate segmentation and somitogenesis. *Cell* **91,** 639–648 (1997).
3. McGrew, M. J., Dale, J. K., Fraboulet, S. & Pourquie, O. The lunatic fringe gene is a target of the molecular clock linked to somite segmentation in avian embryos. *Curr. Biol.* **8,** 979–982 (1998).
4. Forsberg, H., Crozet, F. & Brown, N. A. Waves of mouse Lunatic fringe expression, in four-hour cycles at two-hour intervals, precede somite boundary formation. *Curr. Biol.* **8,** 1027–1030 (1998).
5. Jiang, Y. J. *et al.* Notch signalling and the synchronization of the somite segmentation clock. *Nature* **408,** 475–479 (2000).
6. Bessho, Y. *et al.* Dynamic expression and essential functions of Hes7 in somite segmentation. *Genes Dev.* **15,** 2642–2647 (2001).
7. Saga, Y. & Takeda, H. The making of the somite: molecular events in vertebrate segmentation. *Nature Rev. Genet.* **2,** 835–845 (2001).
8. Pourquie, O. The segmentation clock: converting embryonic time into spatial pattern. *Science* **301,** 328–330 (2003).
9. Saga, Y., Hata, N., Koseki, H. & Taketo, M. M. Mesp2: a novel mouse gene expressed in the presegmented mesoderm and essential for segmentation initiation. *Genes Dev.* **11,** 1827–1839 (1997).
10. Buchberger, A., Seidl, K., Klein, C., Eberhardt, H. & Arnold, H. H. cMeso-1, a novel bHLH transcription factor, is involved in somite formation in chicken embryos. *Dev. Biol.* **199,** 201–215 (1998).
11. Sparrow, D. B. *et al.* Thylacine 1 is expressed segmentally within the paraxial mesoderm of the *Xenopus* embryo and interacts with the Notch pathway. *Development* **125,** 2041–2051 (1998).
12. Sawada, A. *et al.* Zebrafish Mesp family genes, *mesp-a* and *mesp-b* are segmentally expressed in the presomitic mesoderm, and Mesp-b confers the anterior identity to the developing somites. *Development* **127,** 1691–1702 (2000).
13. Takahashi, Y. *et al.* Mesp2 initiates somite segmentation through the Notch signalling pathway. *Nature Genet.* **25,** 390–396 (2000).
14. Bruckner, K., Perez, L., Clausen, H. & Cohen, S. Glycosyltransferase activity of Fringe modulates Notch-Delta interactions. *Nature* **406,** 411–415 (2000).
15. Moloney, D. J. *et al.* Fringe is a glycosyltransferase that modifies Notch. *Nature* **406,** 369–375 (2000).
16. Dale, J. K. *et al.* Periodic notch inhibition by lunatic fringe underlies the chick segmentation clock. *Nature* **421,** 275–278 (2003).
17. Bessho, Y., Hirata, H., Masamizu, Y. & Kageyama, R. Periodic repression by the bHLH factor Hes7 is an essential mechanism for the somite segmentation clock. *Genes Dev.* **17,** 1451–1456 (2003).
18. Hrabe de Angelis, M., McIntyre, J. II & Gossler, A. Maintenance of somite borders in mice requires the Delta homologue Dll1. *Nature* **386,** 717–721 (1997).
19. Evrard, Y. A., Lun, Y., Aulehla, A., Gan, L. & Johnson, R. L. lunatic fringe is an essential mediator of somite segmentation and patterning. *Nature* **394,** 377–381 (1998).
20. Cole, S. E., Levorse, J. M., Tilghman, S. M. & Vogt, T. F. Clock regulatory elements control cyclic expression of Lunatic fringe during somitogenesis. *Dev. Cell* **3,** 75–84 (2002).
21. Morales, A. V., Yasuda, Y. & Ish-Horowicz, D. Periodic Lunatic fringe expression is controlled during segmentation by a cyclic transcriptional enhancer responsive to notch signaling. *Dev. Cell* **3,** 63–74 (2002).
22. Bessho, Y. *et al.* Dynamic expression and essential functions of Hes7 in somite segmentation. *Genes Dev.* **15,** 2642–2647 (2001).
23. Sawada, A. *et al.* Fgf/MAPK signalling is a crucial positional cue in somite boundary formation. *Development* **128,** 4873–4880 (2001).
24. Dubrulle, J., McGrew, M. J. & Pourquie, O. FGF signaling controls somite boundary position and regulates segmentation clock control of spatiotemporal Hox gene activation. *Cell* **106,** 219–232 (2001).
25. Panin, V. M., Papayannopoulos, V., Wilson, R. & Irvine, K. D. Fringe modulates Notch–ligand interactions. *Nature* **387,** 908–912 (1997).
26. Haines, N. & Irvine, K. D. Glycosylation regulates Notch signalling. *Nature Rev. Mol. Cell Biol.* **4,** 786–797 (2003).
27. Hicks, C. *et al.* Fringe differentially modulates Jagged1 and Delta1 signalling through Notch1 and Notch2. *Nature Cell Biol.* **2,** 515–520 (2000).
28. Moreno, T. A. & Kintner, C. Regulation of segmental patterning by retinoic acid signaling during *Xenopus* somitogenesis. *Dev. Cell* **6,** 205–218 (2004).
29. Sakai, Y. *et al.* The retinoic acid-inactivating enzyme CYP26 is essential for establishing an uneven distribution of retinoic acid along the anterio-posterior axis within the mouse embryo. *Genes Dev.* **15,** 213–225 (2001).
30. Nagai, T. *et al.* A variant of yellow fluorescent protein with fast and efficient maturation for cell-biological applications. *Nature Biotechnol.* **20,** 87–90 (2002).

Supplementary Information is linked to the online version of the paper at www.nature.com/nature.

Acknowledgements We thank S. Kitajima and E. Ikeno for their assistance in generating the *Mesp2–venus* knock-in mouse; M. Ikumi and Y. Takahashi for technical assistance and maintaining the mice used in this study; A. Gossler and R. Johnson for providing the Dll1and lunatic fringe knockout mice; and H. Hamada for *CYP26a*-null embryos. We also thank H. Takeda for critical reading of this manuscript. We are grateful to H. Tanaka for preparing purified Mesp2 protein. This work was supported by Grants-in-Aid for Science Research on Priority Areas (B), the Organized Research Combination System and National BioResource Project of the Ministry of Education, Culture, Sports, Science and Technology, Japan.

Author Information Reprints and permissions information is available at npg.nature.com/reprintsandpermissions. The authors declare no competing financial interests. Correspondence and requests for materials should be addressed to Y.S. (ysaga@lab.nig.ac.jp).

© 2005 Nature Publishing Group